J. Ocean Univ. China (Oceanic and Coastal Sea Research)
DOI 10.1007/s11802-016-2837-8
ISSN 1672-5182, 2016 15 (4): 619-626
http://www.ouc.edu.cn/xbywb/
E-mail:xbywb@ouc.edu.cn

Wave Interaction with a Partially Reflecting Vertical Wall Protected by a Submerged Porous Bar

ZHAO Yang, LIU Yong*, and LI Huajun

Shandong Provincial Key Laboratory of Ocean Engineering, *Ocean University of China*, *Qingdao* 266100, *P. R. China*

(Received December 23, 2014; revised March 9, 2015; accepted March 22, 2016)

Abstract This study gives an analytical solution for wave interaction with a partially reflecting vertical wall protected by a submerged porous bar based on linear potential theory. The whole study domain is divided into multiple sub-regions in relation to the structures. The velocity potential in each sub-region is written as a series solution by the separation of variables. A partially reflecting boundary condition is used to describe the partial reflection of a vertical wall. Unknown expansion coefficients in the series solutions are determined by matching velocity potentials among different sub-regions. The analytical solution is verified by an independently developed multi-domain boundary element method (BEM) solution and experimental data. The wave run-up and wave force on the partially reflecting vertical wall are estimated and examined, which can be effectively reduced by the submerged porous bar. The horizontal space between the vertical wall and the submerged porous bar is a key factor, which affects the sheltering function of the porous bar. The wave resonance between the porous bar and the vertical wall may disappear when the vertical wall has a low reflection coefficient. The present analytical solution may be used to determine the optimum parameters of structures at a preliminary engineering design stage.

Key words vertical wall; partial reflection; porous bar; analytical solution; wave run-up; wave force

1 Introduction

Vertical breakwaters, seawalls and sea dikes have been widely used for protecting coastlines and wharfs. Vertical structures may be subjected to severe sea waves. A submerged porous bar can be used to provide a sheltering effect for a vertical structure. Moreover, the submerged porous bar (breakwater) can be easily constructed without affecting coastal aesthetic. The wave transformations between submerged porous bars and vertical walls are rather complicated. For practical engineering design, it is significant to well understand the mechanism of wave transformations between vertical walls and submerged porous bars.

Sollitt and Cross (1972) developed a classical porous medium model to examine wave reflection and transmission by a submerged porous rectangular breakwater. Using the porous medium model of Sollitt and Cross (1972), Yu and Chwang (1994) examined wave motion through a two-layer porous breakwater, and Losada *et al.* (1996) developed an analytical solution for oblique wave interaction with a submerged rectangular porous breakwater. Li and Huang (2006) experimentally studied the reflection and transmission coefficients of submerged porous structures with different shapes. Cheng *et al.* (2009) and Jiang *et al.* (2012) numerically examined wave dissipations inside submerged porous structures. Wu *et al.* (2014) simulated the interaction of solitary waves with submerged rectangular porous breakwaters. The preceding studies have shown that a single submerged porous bar (breakwater) can effectively dissipate incident wave energy.

Besides studying submerged porous bars alone, some researchers have examined submerged bars in front of vertical or slope walls. Reddy and Neelamani (2005) numerically and experimentally examined wave forces acting on a vertical seawall protected by a submerged porous bar. Jeng *et al.* (2005) measured wave transformation between a submerged breakwater and a vertical seawall located on a porous seabed. Chen *et al.* (2007) experimentally studied the wave transformation between a submerged porous breakwater and a slope seawall. Zheng *et al.* (2007) developed analytical solutions for wave diffraction and radiation by a submerged solid bar in front of a vertical wall. Recently, Koley *et al.* (2014) used matched eigenfunction expansions to develop analytical solutions for wave trapping by submerged and surface-piercing porous structures in front of vertical walls. Das and Bora (2014) developed an analytical solution for wave reflection by a porous structure with a vertical solid rear wall. In aforementioned studies, water waves were all fully reflected by rear walls.

However, vertical breakwaters or seawalls are often partially reflecting structures in practice. Goda (2010)

* Corresponding author. Tel: 0086-532-66781129
E-mail: liuyong@ouc.edu.cn

gave the approximate reflection coefficients of different coastal structures, as listed in Table 1. It can be seen from Table 1 that the reflection coefficient of a wave-energy-dissipation vertical structure, such as perforated caissons (Huang *et al.*, 2011; Lee and Shin, 2014), may be as low as 0.3. To describe a partially reflecting wall in mathematics, Isaacson and Qu (1990) developed a partially reflecting boundary condition using potential theory. Based on the boundary condition of Isaacson and Qu (1990), Elchahal *et al.* (2008) examined the effects of harbor sidewall reflection on floating breakwaters. They found that the hydrodynamic performance of floating breakwaters was significantly changed by the lee side partially reflecting wall.

The objective of this study is to develop an analytical solution for wave interaction with a partially reflecting wall protected by an idealized rectangular porous bar. The engineering background of the present study is to construct an offshore submerged rubble mound breakwater for protecting wave-energy-dissipation vertical seawalls or sea dikes (such as perforated caissons). In the following section, the mathematical model of the present problem is formulated and solved using matched eigenfunction expansions. In Section 3, the analytical solution is verified by experimental data and an independently developed multi-domain boundary element method (BEM) solution. In Section 4, selected numerical examples are presented to examine the wave run-up and wave force on the vertical wall and the results are presented as reference for practical engineering. Finally, the main conclusions of this study are drawn.

Table 1 Approximate reflection coefficients for various coastal structures (Goda, 2010)

Coastal structure	Reflection coefficient
Vertical wall with crown above water	0.7–1.0
Vertical wall with submerged crown	0.5–0.7
Slope of rubble stones(slope of 1 on 2 to 3)	0.3–0.6
Slope of energy dissipating concrete blocks	0.3–0.5
Vertical structure of energy dissipating type	0.3–0.8
Natural beach	0.05–0.2

2 Mathematical Model

The wave interaction with a partially reflecting vertical wall protected by a submerged porous bar is sketched in Fig.1. A Cartesian coordinate system, with the origin located on the still water level and the z-axis directing upwards along the vertical midline of the porous bar, is used for mathematical descriptions. The porous bar with a width of B (B=2b) and a thickness of a is submerged in sea water with a finite depth of h. The submerged depth of the porous bar is d and thus h=d+a. The horizontal space between the bar rear face and the partially reflecting vertical wall is D. The reflection coefficient of the vertical wall is K_r. The whole fluid domain is divided into four regions: region 1, the fluid domain in front of the porous bar; region 2, the fluid domain above the porous bar; region 3, the fluid domain occupied by the porous bar; and region 4, the fluid domain between the porous bar and the vertical wall.

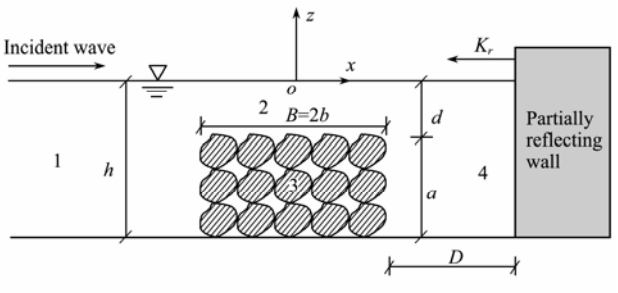

Fig.1 Sketch of wave interaction with a partially reflecting wall protected by a submerged porous bar.

The mathematical model is based on the linear potential theory. Following the classical porous medium model of Sollitt and Cross (1972), the porous bar is regarded as a rigid and homogenous porous medium. Then, the effects of porous medium on fluid motion are represented by three parameters: the linearized resistance coefficient f, the inertial coefficient s, and the porosity ε. The fluid motions inside and outside the porous bar can both be described by a velocity potential $\Phi(x, z, t)$. For harmonic incident waves with angular frequency ω, the time factor $\exp(-\mathrm{i}\omega t)$ can be separated from the velocity potential:

$$\Phi(x,z,t)=\mathrm{Re}\left[\phi(x,z)\mathrm{e}^{-\mathrm{i}\omega t}\right], \tag{1}$$

where Re means the real part of variables in the square brackets, ϕ is the complex spatial velocity potential, and $\mathrm{i}=\sqrt{-1}$.

The spatial velocity potential satisfies the Laplace equation in each region:

$$\frac{\partial^2\phi_j}{\partial x^2}+\frac{\partial^2\phi_j}{\partial z^2}=0, \quad j=1,2,3,4. \tag{2}$$

where the subscript j denotes the variables in region j. On the free surface, the water bottom, the upper horizontal face of the bar, and the far field, the velocity potentials satisfy the following boundary conditions:

$$\frac{\partial\phi_j}{\partial z}=\frac{\omega^2}{g}\phi_j,\ z=0,\ j=1,2,4, \tag{3}$$

$$\frac{\partial\phi_j}{\partial z}=0,\ z=-h,\ j=1,3,4, \tag{4}$$

$$\frac{\partial\phi_2}{\partial z}=\varepsilon\frac{\partial\phi_3}{\partial z},\ -b\le x\le b,\ z=-d, \tag{5a}$$

$$\phi_2=(s+\mathrm{i}f)\phi_3,\ -b\le x\le b,\ z=-d, \tag{5b}$$

$$\lim_{x\to-\infty}\left(\frac{\partial}{\partial x}+\mathrm{i}k_0\right)(\phi_1-\phi_0)=0, \tag{6}$$

where g is the gravitational acceleration, k_0 is the incident wave number, and ϕ_0 is the velocity potential of incident waves given by

$$\phi_0=-\frac{\mathrm{i}gH}{2\omega}\frac{\cosh k_0(z+h)}{\cosh k_0 h}\mathrm{e}^{\mathrm{i}k_0 x}, \tag{7}$$

where H is the incident wave height.

The velocity potentials, which satisfy the Laplace equation (Eq. (2)) and the relevant boundary conditions in Eqs. (3)–(6), can be written as

$$\phi_1=-\frac{\mathrm{i}gH}{2\omega}\Big[\mathrm{e}^{\mathrm{i}k_0(x+b)}Z_0(z)+R_0\,\mathrm{e}^{-\mathrm{i}k_0(x+b)}Z_0(z)+\sum_{m=1}^{\infty}R_m\,\mathrm{e}^{k_m(x+b)}Z_m(z)\Big], \tag{8}$$

$$\phi_2=-\frac{\mathrm{i}gH}{2\omega}\sum_{m=0}^{\infty}\Big[A_m\cos(\lambda_m x)U_m(z)+B_m\sin(\lambda_m x)U_m(z)\Big], \tag{9}$$

$$\phi_3=-\frac{\mathrm{i}gH}{2\omega}\sum_{m=0}^{\infty}\Big[A_m\cos(\lambda_m x)V_m(z)+B_m\sin(\lambda_m x)V_m(z)\Big], \tag{10}$$

$$\phi_4=-\frac{\mathrm{i}gH}{2\omega}\Big[C_0\,\mathrm{e}^{\mathrm{i}k_0(x-b)}Z_0(z)+D_0\,\mathrm{e}^{-\mathrm{i}k_0(x-b-D)}Z_0(z)+\sum_{m=1}^{\infty}C_m\,\mathrm{e}^{-k_m(x-b)}Z_m(z)+\sum_{m=1}^{\infty}D_m\,\mathrm{e}^{k_m(x-b-D)}Z_m(z)\Big], \tag{11}$$

where R_m, A_m, B_m, C_m and D_m are the unknown expansion coefficients; and $Z_m(z)$, $U_m(z)$ and $V_m(z)$ are the vertical eigenfunctions defined as

$$Z_0(z)=\frac{\cosh k_0(z+h)}{\cosh k_0 h}, \tag{12a}$$

$$Z_m(z)=\frac{\cos k_m(z+h)}{\cos k_m h},\ m=1,2,\cdots, \tag{12b}$$

$$U_m(z)=\frac{\cosh\lambda_m(z+h)-P_m\sinh\lambda_m(z+h)}{\cosh\lambda_m h-P_m\sinh\lambda_m h}, \tag{13}$$

$$V_m(z)=\frac{1-P_m\tanh\lambda_m a}{s+\mathrm{i}f}\frac{\cosh\lambda_m(z+h)}{\cosh\lambda_m h-P_m\sinh\lambda_m h}, \tag{14}$$

$$P_m=\frac{\left[1-\varepsilon/(s+\mathrm{i}f)\right]\tanh\lambda_m a}{1-\varepsilon/(s+\mathrm{i}f)\tanh^2\lambda_m a}. \tag{15}$$

The eigenvalues k_m are positive real roots in the following wave dispersion relations:

$$\omega^2=gk_0\tanh k_0 h=-gk_m\tan k_m h,\ m=1,2,\cdots, \tag{16}$$

The eigenvalues λ_m satisfy the following complex dispersion relations:

$$\omega^2-g\lambda_m\tanh\lambda_m h=P_m\left[\omega^2\tan\lambda_m h-g\lambda_m\right]. \tag{17}$$

All the complex roots of Eq. (17) are found using the Newton-Raphson method, and the initial guesses of the roots are determined by the perturbation method of Mendez and Losada (2004).

It is noted that the wave number k_0 is corresponding to propagation waves. However, the eigenvalues k_m (m=1, 2, ⋯) are corresponding to a series of evanescent modes, which decay exponentially with the increasing distance from structures.

On the common boundaries of different regions (x=±b), the velocity potential and the horizontal mass fluxes must be continuous:

$$\phi_1=\phi_2,\ x=-b,\ -d\le z\le 0, \tag{18a}$$

$$\phi_1=(s+\mathrm{i}f)\phi_3,\ x=-b,\ -h\le z<-d, \tag{18b}$$

$$\frac{\partial\phi_1}{\partial x}=\frac{\partial\phi_2}{\partial x},\ x=-b,\ -d\le z\le 0, \tag{19a}$$

$$\frac{\partial\phi_1}{\partial x}=\varepsilon\frac{\partial\phi_3}{\partial x},\ x=-b,\ -h\le z<-d, \tag{19b}$$

$$\phi_4=\phi_2,\ x=b,\ -d\le z\le 0, \tag{20a}$$

$$\phi_4=(s+\mathrm{i}f)\phi_3,\ x=b,\ -h\le z<-d, \tag{20b}$$

$$\frac{\partial\phi_4}{\partial x}=\frac{\partial\phi_2}{\partial x},\ x=b,\ -d\le z\le 0, \tag{21a}$$

$$\frac{\partial\phi_4}{\partial x}=\varepsilon\frac{\partial\phi_3}{\partial x},\ x=b,\ -h\le z<-d. \tag{21b}$$

On the vertical wall, the partially reflecting boundary condition is given by Isaacson and Qu (1990):

$$\frac{\partial\phi_4}{\partial x}=\mathrm{i}\frac{1-K_r}{1+K_r}k_0\phi_4,\ x=b+D, \tag{22}$$

where K_r is the reflection coefficient of the vertical wall (Fig.1). When K_r is unity, transmitted waves by the porous bar are totally reflected by the vertical wall; when K_r is zero, transmitted propagation waves are totally dissipated by the vertical wall. Eq. (22) was originally developed in the context of plane waves, and the effects of evanescent modes were not included. Thus, for K_r = 0 at a small value of D, the boundary condition in Eq. (22) does not become a far field radiation condition due to the existence of evanescent modes near the vertical wall. This may be reasonable in practice. It is also noted that the reflection coefficient of a coastal structure is defined as the ratio of the reflected wave height to the incident wave height. On the right hand side of Eq. (11), the first and second part denote waves propagating along the positive and negative x-direction, respectively. Thus,

$$K_r=\left|\frac{D_0}{C_0}\right|, \tag{23}$$

which can be used as a benchmark for this analytical so-

lution.

The unknown expansion coefficients in Eqs. (8)–(11) are determined using the boundary conditions in Eqs. (18)–(22). For example, substituting the velocity potentials in Eqs. (8) and (9) into Eq. (18), it yields:

$$Z_0(z)+\sum_{m=0}^{\infty}R_m Z_m(z)=\sum_{m=0}^{\infty}\left[A_m\cos\lambda_m b-B_m\sin\lambda_m b\right]U_m(z),\quad -d\le z\le 0, \tag{24a}$$

$$Z_0(z)+\sum_{m=0}^{\infty}R_m Z_m(z)=\sum_{m=0}^{\infty}\left[A_m\cos\lambda_m b-B_m\sin\lambda_m b\right](s+\mathrm{i}f)V_m(z),\quad -h\le z<-d. \tag{24b}$$

Multiplying both sides of Eq. (24) by $Z_n(z)$, integrating with respect to z from $-h$ to 0, and then using the orthogonality of $Z_n(z)$ and truncating n and m after N terms, we have

$$\{e_n\}_{(N+1)}+\{R_n\}_{(N+1)}=[a_{nm}]_{(N+1)\times(N+1)}\{A_m\}_{(N+1)}+[b_{nm}]_{(N+1)\times(N+1)}\{B_m\}_{(N+1)}, \tag{25}$$

where the matrix coefficients are listed in Table 2. Using the similar method to the above, we can transform Eqs. (19)–(22) into

$$-\{e_n\}_{(N+1)}+\{R_n\}_{(N+1)}=[c_{nm}]_{(N+1)\times(N+1)}\{A_m\}_{(N+1)}+[d_{nm}]_{(N+1)\times(N+1)}\{B_m\}_{(N+1)}, \tag{26}$$

$$\{C_n\}_{(N+1)}+\mathrm{e}^{-\tilde{k}_n D}\{D_n\}_{(N+1)}=[a_{nm}]_{(N+1)\times(N+1)}\{A_m\}_{(N+1)}-[b_{nm}]_{(N+1)\times(N+1)}\{B_m\}_{(N+1)}, \tag{27}$$

$$-\{C_n\}_{(N+1)}+\mathrm{e}^{-\tilde{k}_n D}\{D_n\}_{(N+1)}=-[c_{nm}]_{(N+1)\times(N+1)}\{A_m\}_{(N+1)}+,\ [d_{nm}]_{(N+1)\times(N+1)}\{B_m\}_{(N+1)}, \tag{28}$$

$$\left(\alpha k_0+\tilde{k}_n\right)\mathrm{e}^{-\tilde{k}_n D}\{C_n\}_{(N+1)}+\left(\alpha k_0-\tilde{k}_n\right)\{D_n\}_{(N+1)}=0, \tag{29}$$

where the matrix coefficients are also listed in Table 2. Eqs. (25)–(29) are simultaneously solved by Gauss elimination method. Then, all the unknown expansion coefficients are determined and various hydrodynamic quantities of engineering interests can be estimated.

The reflection coefficient of the system of porous bar and the vertical wall is calculated by

$$C_R=|R_0|. \tag{30}$$

The surface elevation on the vertical wall is estimated by

$$\eta=\frac{\mathrm{i}\omega}{g}\phi_4(b+D,0)=\frac{H}{2}\left(\sum_{m=0}^{\infty}C_m\mathrm{e}^{-\tilde{k}_m D}+\sum_{m=0}^{\infty}D_m\right). \tag{31}$$

The dimensionless wave run-up on the vertical wall is defined as

$$C_H=\frac{2|\eta|}{H}. \tag{32}$$

The dynamic pressure on the vertical wall is calculated by the linear Bernoulli equation

$$p(b+D,z)=\mathrm{i}\rho\omega\phi(b+D,z),$$

where ρ is the water density. Integrating the dynamic pressure along the vertical wall, we get the magnitude of horizontal wave force acting on the wall:

$$F=\mathrm{i}\rho\omega\int_{-h}^{0}\phi_4(b+D,z)\,\mathrm{d}z=\frac{\rho g H}{2}\left[\left(C_0\mathrm{e}^{\mathrm{i}k_0 D}+D_0\right)\frac{\tanh k_0 h}{k_0}+\sum_{m=1}^{\infty}\left(C_m\mathrm{e}^{-k_m D}+D_m\right)\frac{\tan k_m h}{k_m}\right]. \tag{33}$$

The dimensionless horizontal wave force on the vertical wall is defined as

$$C_F=\frac{|F|}{\rho g H h}. \tag{34}$$

Table 2 The matrix coefficients in Eqs. (25)–(29)

Coefficient	Value
e_n	$1\ (n=0),\ 0\ (n\neq 0)$
a_{nm}	$\cos(\lambda_m b)\frac{\Lambda_{mn}+(s+\mathrm{i}f)\Omega_{mn}}{\Gamma_n}$
b_{nm}	$-\sin(\lambda_m b)\frac{\Lambda_{mn}+(s+\mathrm{i}f)\Omega_{mn}}{\Gamma_n}$
c_{nm}	$\lambda_m\sin(\lambda_m b)\frac{\Lambda_{mn}+\varepsilon\Omega_{mn}}{\tilde{k}_n\Gamma_n}$
d_{nm}	$\lambda_m\cos(\lambda_m b)\frac{\Lambda_{mn}+\varepsilon\Omega_{mn}}{\tilde{k}_n\Gamma_n}$
$\tilde{k}_n$	$-\mathrm{i}k_0\ (n=0),\ k_n(n\neq 0)$
Λ_{mn}	$\int_{-d}^{0}U_m(z)Z_n(z)\,\mathrm{d}z$
Ω_{mn}	$\int_{-h}^{-d}V_m(z)Z_n(z)\,\mathrm{d}z$
Γ_n	$\int_{-h}^{0}Z_n^2(z)\,\mathrm{d}z$

3 Validation

3.1 Convergence Examination

For the present series solution, the truncated number N must be carefully determined for obtaining convergent results. Table 3 lists the calculated results for the dimensionless wave run-up C_H and the dimensionless wave force C_F at different N values for a typical case with $k_0 d$=1.2, B/h=1.2, D/h=3.0, ε=0.4, f=2.0, s=1.0 and K_r=0.8. It can be seen that the truncated number N=40 is sufficient to ensure accurate results for engineering purposes and thus, is used in the present study.

Table 3 Convergence of C_H and C_F with increasing truncated number N

Truncated number N	a/h=0.1		a/h=0.2		a/h=0.5		a/h=0.95	
	C_H	C_F	C_H	C_F	C_H	C_F	C_H	C_F
2	1.8055	0.6272	1.7943	0.6233	1.5764	0.5476	0.2943	0.1022
5	1.8024	0.6261	1.7822	0.6190	1.5792	0.5485	0.2647	0.0920
10	1.8013	0.6257	1.7819	0.6190	1.5774	0.5479	0.2568	0.0892
20	1.8012	0.6257	1.7819	0.6189	1.5774	0.5479	0.2541	0.0882
40	1.8012	0.6257	1.7818	0.6189	1.5774	0.5479	0.2541	0.0883
60	1.8012	0.6256	1.7818	0.6189	1.5774	0.5479	0.2541	0.0883

3.2 The Special Case of a Single Submerged Porous Bar

If the reflection coefficient K_r of the vertical wall is zero and the distance D between the porous bar and the vertical wall is large, the partially reflection boundary condition on the vertical wall will become a far field radiation condition. Then, the present problem will reduce to that of wave motion over a single submerged porous bar. For this special case, the calculated results of D_m (m= 0, 1, 2, ⋯) in Eq. (11) are all zero, and the transmission coefficient of the porous bar can be calculated by

$$C_T = |C_0| . \tag{35}$$

Li and Huang (1996) measured the reflection and transmission coefficients of a submerged rectangular porous bar by a series of model tests. Here the reflection and transmission coefficients predicted by the present analytical solution are compared with the experimental data of Li and Huang (1996). For such practical calculations, the values of three parameters ε, f and s must be known. The value of ε was 0.678 in the tests of Li and Huang (1996). According to Pérez-Romero *et al.* (2009), the inertial coefficient s is simply assumed as unity, and the resistance coefficient f is calculated by

$$f = 0.46\left(D_s k_0\right)^{-0.57} , \tag{36}$$

where D_s is the nominal diameter of stones and D_s = 1.95 cm in the tests of Li and Huang (1996). The water depth used in Li and Huang (1996) was 30 cm.

The comparisons between the present predictions and the experimental data of Li and Huang (1996) at different values of a/h and B/h are given in Figs.2–4. It can be seen from these figures that the agreement between the analytical solution and the experimental data is reasonable. This means that the present solution may be acceptable for practical problems.

3.3 Comparison with Multi-Domain BEM Solution

To confirm the analytical solution, we have developed a multi-domain BEM solution for the present boundary value problem. The multi-domain BEM solution is slightly modified by the solution of Liu *et al.* (2012). The fundamental solution of Laplace equation, which does not satisfy any boundary condition, is adopted. All the boundary curves are discretized using constant elements. However,

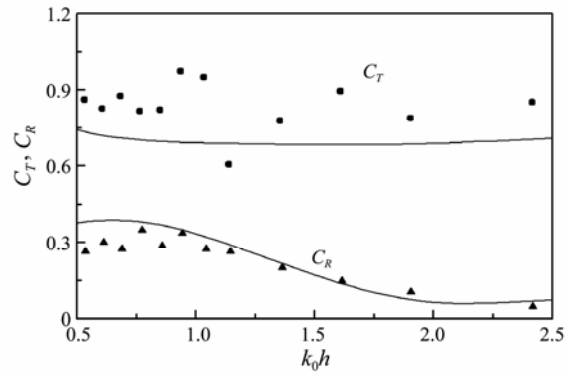

Fig.2 Comparison between the present analytical solution (lines) and the experimental results of Li and Huang (1996) (dots) at a/h=0.751 and B/h=0.634.

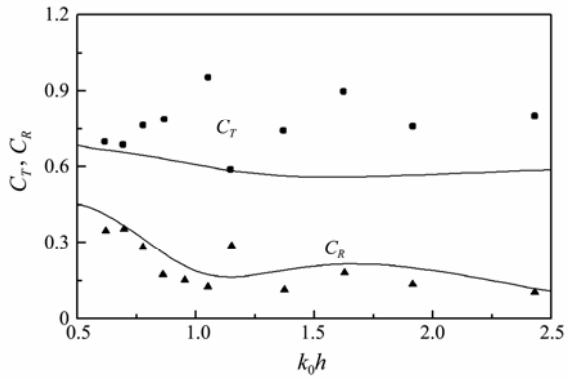

Fig.3 Comparison between the present analytical solution (lines) and the experimental results of Li and Huang (1996) (dots) at a/h=0.751 and B/h=1.268.

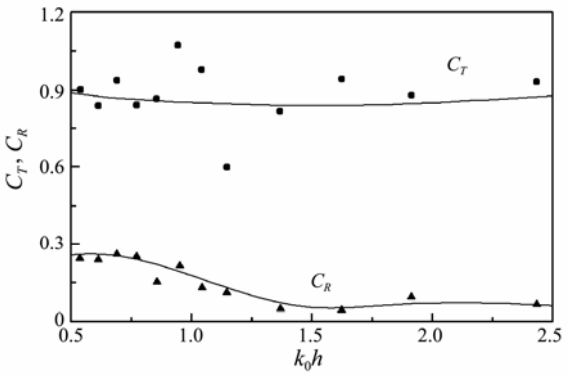

Fig.4 Comparison between the present analytical solution (lines) and the experimental results of Li and Huang (1996) (dots) at a/h=0.495 and B/h=1.268.

the far field radiation condition at the lee side of the structure in Liu *et al.* (2012) is replaced by the present partially reflecting boundary condition in Eq. (22). Numerically the multi-domain BEM solution is cumbersome, and all the boundaries of the fluid domain need to be discretized. However, the BEM solution can be suitable to submerged porous bars with complicated shapes.

The reflection coefficient C_R and the wave run-up C_H calculated by the present analytical solution and the multi-domain BEM solution are compared for a typical case in Fig.5. With a/h=0.5, B/h=1.0, D/h=1.0, ε=0.45, f=2.0, s=1.0 and K_r=0.5, it is evident that the agreement between the two different solutions is excellent. In addition, the calculated results of D_0 and C_0 by the analytical solution satisfy the relation in Eq. (23), which verifies the correctness of the solution procedure of the present analytical solution.

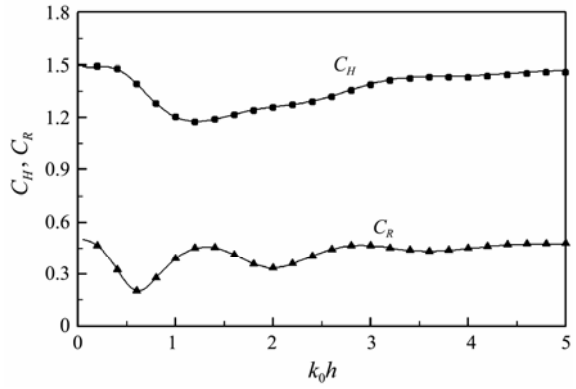

Fig.5 Comparison between the present analytical solution (lines) and the multi-domain BEM solution (dots).

4 Results and Discussion

We first examine the effects of relative porous bar thickness a/h on the dimensionless wave run-up C_H and the dimensionless wave force C_F on the vertical wall. The results are presented in Figs.6 and 7 by setting B/h=1.2, D/h=3.0, ε=0.4, f=2.0, s=1.0 and K_r=0.5. In these figures, the case of a/h=0 denotes that no obstacle exists in front of the partially reflecting vertical wall. When the thickness of the porous bar increases, both the wave run-up and the wave force on the vertical wall decrease. The decrease of wave run-up may reduce the potential wave overtopping on the vertical wall, and the decrease of horizontal wave force enhances the stability of the vertical wall. Thus, the submerged porous bar can provide effective sheltering for the partially reflecting vertical wall. It is noted that directly increasing the vertical wall height can also reduce the wave overtopping. But only increasing the vertical wall height may increase the wave forces acting on it while construction of a submerged porous bar is more beneficial for the stability of a vertical wall.

With a/h=0.5, B/h=1.2, D/h=3.0, ε=0.4, f=2.0 and s=1.0, Figs.8 and 9 show the effects of the vertical wall reflection coefficient K_r on the dimensionless wave run-up C_H and the dimensionless wave force C_F, respectively. When the reflection of vertical wall is unity (K_r = 1), waves can be totally reflected by the vertical wall and the wave resonance may occur between the porous bar and the vertical wall. As a result, the dimensionless standing wave height in front of the reflecting vertical wall C_H can be larger than 2.0. Thus, not only the submerged porous bar cannot provide effective sheltering for the vertical wall, but can even increase wave run-up and wave force over the wall, which should be avoided in practical engineering design. However, as the reflection coefficient of the vertical wall decreases, both wave run-up and wave force decrease significantly and wave resonance between the porous bar and the vertical wall disappears.

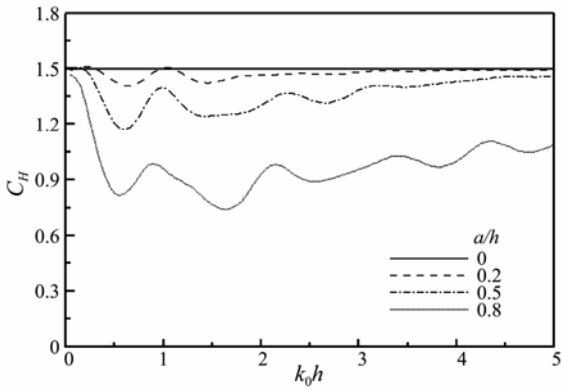

Fig.6 Effect of the relative porous bar thickness a/h on the dimensionless wave run-up C_H over the vertical wall.

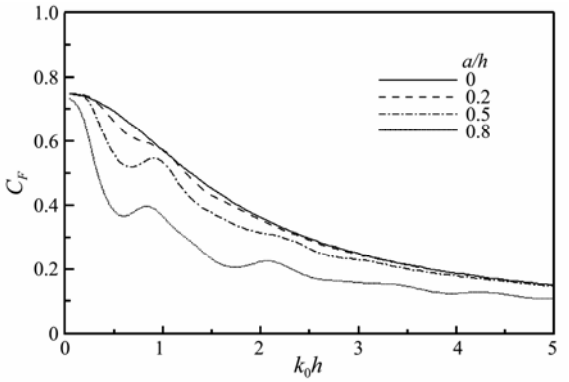

Fig.7 Effect of the relative porous bar thickness a/h on the dimensionless wave force C_F on the vertical wall.

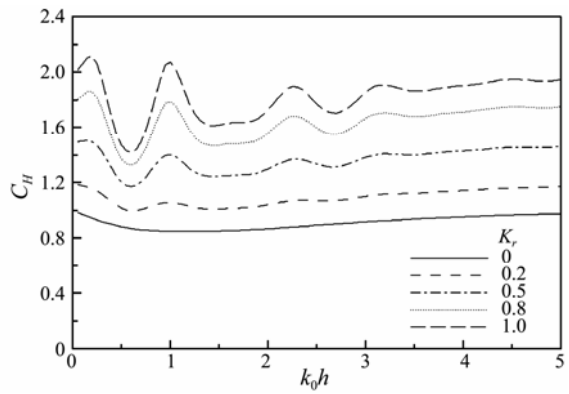

Fig.8 Effect of the vertical wall refection coefficient K_r on the dimensionless wave run-up C_H over the vertical wall.

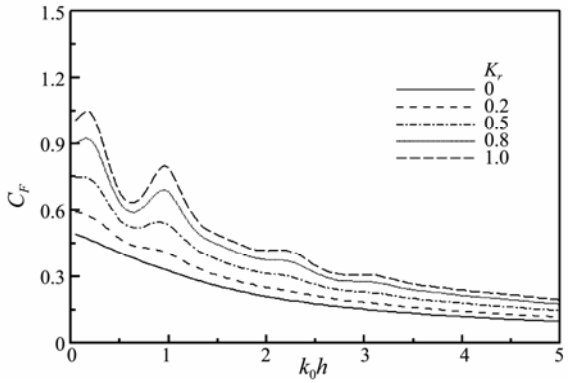

Fig.9 Effect of the vertical wall refection coefficient K_r on the dimensionless wave force C_F on the vertical wall.

Figs.10 and 11 show the effects of the relative space between the submerged porous bar and the vertical wall, D/L, on wave run-up and wave force, respectively. Here, for three relative porous bar widths, B/h=0.5, 1.0 and 1.5, k_0h=1.2, a/h=0.5, ε=0.4, f=2.0, s=1.0 and K_r=0.8. It can be seen from these figures that both wave run-up and wave force vary periodically with the increasing values of D/L. Therefore, to obtain the minimum wave run-up C_H and wave force C_F, a value of D/L (D/L≈0.3, 0.75 and 1.35) ought to be carefully chosen. Also, it can be seen from Figs.10 and 11 that the minimum values of wave run-up and wave force are close for different porous bar widths. This means that to obtain lower C_H and C_F, only increasing the porous bar width will increase engineering cost and would be inadvisable.

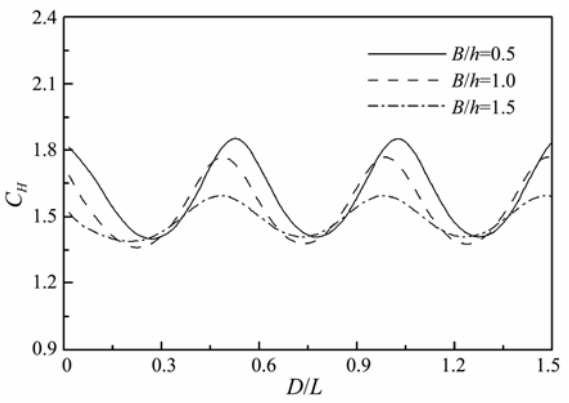

Fig.10 Effect of the relative space D/L between the porous bar and the vertical wall on the dimensionless wave run-up C_H over the vertical wall.

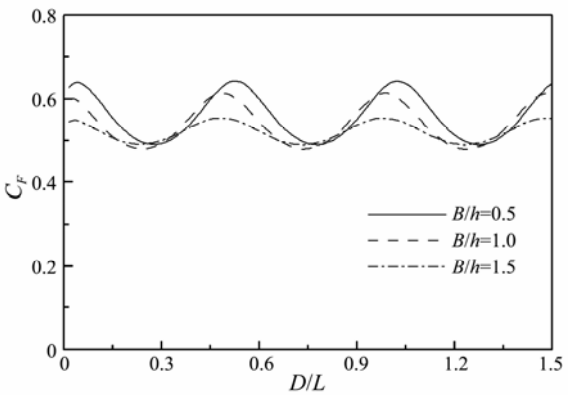

Fig.11 Effect of the relative space D/L between the porous bar and the vertical wall on the dimensionless wave force C_F on the vertical wall.

Figs.12 and 13 show the variations of the dimensionless wave run-up C_H and the dimensionless wave force C_F with the relative porous bar width B/L at different porosities, respectively. With k_0h=1.2, a/h=0.5, D/h=3.0, f=2.0, s=1.0 and K_r=0.8, the case of ε=0 shows that a submerged solid bar cannot dissipate additional wave energy. As a result, both wave run-up and wave force vary periodically with the increase of B/L. As the porosity ε increases, the values of C_F and C_H both decrease due to the increasing wave energy dissipation by the porous bar. It should be mentioned that the practical values of porosity ε for rubble mounds are about 0.35−0.5. The case of ε = 0.8 can only be obtained by using artificial concrete blocks. Also it can be seen from Figs.12 and 13 that for a submerged porous bar, the values of C_F and C_H both decrease with the increase of relative bar width B/L. This means that a wider porous bar can dissipate more wave energy, but lead to a higher engineering cost. Figs.10−13 indicate that it is very important to carefully specify the values D and B for efficient engineering design. The present analytical solution can be used for finding the optimum values of D and B at a preliminary design stage.

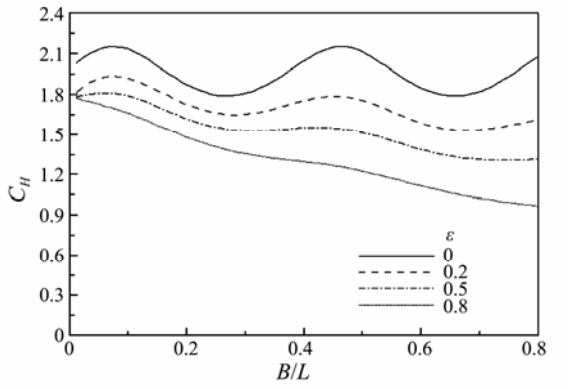

Fig.12 Effect of the relative bar width B/L on the dimensionless wave run-up C_H over the vertical wall.

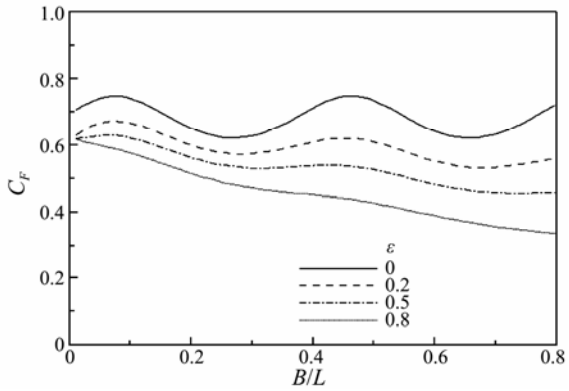

Fig.13 Effect of the relative bar width B/L on the dimensionless wave force C_F on the vertical wall.

5 Concluding Remarks

An analytical solution is developed in the present paper for wave interaction with a partially reflecting vertical wall protected by a submerged porous bar. The matched eigenfunction expansions are used to obtain the solution, which is confirmed by an independently developed multi-domain BEM solution for the same problem and a series of experimental data for a single submerged porous bar. The truncated number of N=40 in the present series solution is proved to be sufficient large for obtaining convergent results. The wave run-up and the wave force over the partially reflecting vertical wall are examined by numerical examples.

A submerged porous bar can effectively reduce the wave run-up and the wave force over a partially reflecting vertical wall. The wave resonance may occur between a fully reflecting vertical wall and a submerged porous bar. But the wave resonance disappears when the reflection coefficient of the vertical wall is small. The increase of porosity or relative width of a porous bar can increase the wave energy dissipation. The space between the vertical wall and the submerged porous bar is a key factor to affect the wave run-up and the wave force on the vertical wall. The optimum space between the porous bar and the vertical wall may be determined using the present analytical solution.

Acknowledgements

This study was supported by the National Natural Science Foundation of China (Project Nos. 51322903 and 51279224), and the Program for New Century Excellent University Talents in University (NCET-13-0528).

References

Chen, H. B., Tsai, C. P., and Jeng, C. C., 2007. Wave transformation between submerged breakwater and seawall. *Journal of Coastal Research*, **23** (1): 1069-1074.

Cheng, Y. Z., Jiang, C. B., and Wang, Y. Y., 2009. A coupled numerical model of wave interaction with porous medium. *Ocean Engineering*, **36** (12): 952-959.

Das, S., and Bora, S. N., 2014. Reflection of oblique ocean water waves by a vertical porous structure placed on a multi-step impermeable bottom. *Applied Ocean Research*, **47**: 373-385.

Elchahal, G., Younes, R., and Lafon, P., 2008. The effects of reflection coefficient of the harbour sidewall on the performance of floating breakwaters. *Ocean Engineering*, **35** (11): 1102-1112.

Goda, Y., 2010. *Random Seas and Design of Maritime Structures*. World Scientific Publishing Company, 732pp.

Huang, Z., Li, Y., and Liu, Y., 2011. Hydraulic performance and wave loadings of perforated/slotted coastal structures: A review. *Ocean Engineering*, **38** (10): 1031-1053.

Isaacson, M., and Qu, S., 1990. Waves in a harbour with partially reflecting boundaries. *Coastal Engineering*, **14** (3): 193-214.

Jeng, D. S., Schacht, C., and Lemckert, C., 2005. Experimental study on ocean waves propagating over a submerged breakwater in front of a vertical seawall. *Ocean Engineering*, **32** (17): 2231-2240.

Jiang, C. B., Cheng, Y. Z., Chang, L. H., and Xia, B., 2012. The numerical study of wave-induced pore water pressure response in highly permeable seabed. *Acta Oceanologica Sinica*, **31** (6): 46-55.

Koley, S., Behera, H., and Sahoo, T., 2014. Oblique wave trapping by porous structures near a wall. *Journal of Engineering Mechanics*, DOI: 10.1061/(ASCE)EM.1943-7889.0000843.

Lee, J. I., and Shin, S. W., 2014. Experimental study on the wave reflection of partially perforated wall caisson with single and double chambers. *Ocean Engineering*, **91**: 1-10.

Li, Z., and Huang, X., 1996. Wave Interaction with submerged porous structures. *Proceedings of the 17th Ocean Engineering Conference*, Taiwan, 273-280 (in Chinese with English abstract).

Liu, Y., Li, H. J., and Li, Y. C., 2012. A new analytical solution for wave scattering by a submerged horizontal porous plate with finite thickness. *Ocean Engineering*, **42**: 83-92.

Losada, I. J., Silva, R., and Losada, M. A., 1996. 3-D non-breaking regular wave interaction with submerged breakwaters. *Coastal Engineering*, **28** (1): 229-248.

Mendez, F. J., and Losada, I. J., 2004. A perturbation method to solve dispersion equations for water waves over dissipative media. *Coastal Engineering*, **51**: 81-89.

Pérez-Romero, D. M., Ortega-Sánchez, M., Moñino, A., and Losada, M. A., 2009. Characteristic friction coefficient and scale effects in oscillatory porous flow. *Coastal Engineering*, **56** (9): 931-939.

Reddy, M. G., and Neelamani, S., 2005. Hydrodynamic studies on vertical seawall defenced by low-crested breakwater. *Ocean Engineering*, **32** (5): 747-764.

Sollitt, C. K., and Cross, R. H., 1972. Wave transmission through permeable breakwaters. *Proceedings of the 13th Coastal Engineering Conference*, Vancouver, 1827-1846.

Wu, Y. T., Yeh, C. L., and Hsiao, S. C., 2014. Three-dimensional numerical simulation on the interaction of solitary waves and porous breakwaters. *Coastal Engineering*, **85**: 12-29.

Yu, X., and Chwang, A. T., 1994. Wave motion through porous structures. *Journal of Engineering Mechanics*, **120** (5): 989-1008.

Zheng, Y. H., Shen, Y. M., and Tang, J., 2007. Radiation and diffraction of linear water waves by an infinitely long submerged rectangular structure parallel to a vertical wall. *Ocean Engineering*, **34** (1): 69-82.

(Edited by Xie Jun)